

Epitaxial growth of quaterphenyl thin films on gold(111)

S. Müllegger,^{a)} I. Salzmann, R. Resel, and A. Winkler

Institute of Solid State Physics, Graz University of Technology, Petersgasse 16, A-8010 Graz, Austria

(Received 4 August 2003; accepted 8 October 2003)

The crystal structure and molecular arrangement of para-quaterphenyl (4P) grown on single crystalline Au(111) was investigated over a wide thickness range. The molecular arrangement in the first monolayer, as investigated with low energy electron diffraction, shows a highly regular structure. This wetting layer is defined by adsorbate–substrate interactions and forms a prestage for the epitaxial growth of 4P single crystalline islands, as observed in x-ray diffraction. Two similar orientations of the 4P bulk phase are observed, with the (211) and (311) planes parallel to the Au(111) surface. The alignment of the molecules was kept unchanged from the first monolayers up to a film thickness of 200 nm. © 2003 American Institute of Physics. [DOI: 10.1063/1.1631380]

Recently, highly crystalline thin films of organic semiconductors have attracted large interest in the field of organic (opto)electronics.^{1–6} Defined interfaces, the right molecular orientation within a crystalline film and large domain sizes are required to enhance the performance of such devices.^{7,8} In particular, oligo-phenyls have been studied in detail and have proven their applicability in electronic and optoelectronic devices.^{9–13} In this letter we present studies on the structure and epitaxial growth of para-quaterphenyl (C₂₄H₁₈, 4P) thin films on single crystalline Au(111), from the initial stages up to a thickness of 200 nm.

The sample preparation and low energy electron diffraction (LEED) measurements were performed under ultrahigh vacuum conditions (10⁻¹⁰ mbar). The single crystal Au(111) surface was cleaned using conventional sputter/annealing techniques. A home-built Knudsen cell was applied for the 4P film deposition. The films were evaporated at room temperature with a rate of 0.18 nm/min. The mean film thickness was monitored by a water-cooled quartz crystal microbalance during the evaporation process. In combination with thermal desorption spectroscopy (TDS), this allows the preparation of well-defined 4P mono- and multilayer films.¹⁴ An Omicron micro-channelplate low energy electron diffraction instrument (MCP-LEED) was used for crystal structure determination of the 4P monolayer, which allows for low emission current (nA) to prevent potential damage of the organic film by electron bombardment. No significant influence of the Au(111) reconstruction^{15,16} on the 4P monolayer growth was observed.¹⁷

The crystal structure of the 4P bulk was investigated *ex situ* by x-ray diffraction (XRD), performing $\Theta/2\Theta$ scans and pole figures¹⁸ on 30 and 200 nm thick films. A Philips X'Pert texture goniometer with Cr K α radiation was used, allowing investigations in the whole orientation space. The pole figures were taken with an angular resolution of $\Delta\psi=1^\circ$ and $\Delta\varphi=3^\circ$. Simultaneous measurements of the Au(111) substrate and the 4P film were done in order to detect the mutual relationship of the crystalline orientations. Analysis of the diffraction data were performed on the basis of their single

crystal structures^{19,20} by using the software POWDER CELL, STEREOGRAMM, and STEREOPOLE.^{21–23}

Figure 1(a) shows a LEED image of the 4P monolayer on Au(111). Due to a pronounced energy dependence of the spot intensities (extinctions) it was necessary to record a series of LEED images between 15 and 45 V. The positions of the spots in each single LEED image were subsequently corrected for inherent image deformation of the MCP-LEED optics. The corrected spot positions were transferred into a separate representation free of image deformation, as shown in Fig. 1(b). Considering the rotational symmetry and mirror planes of the Au(111) surface, we could explain the LEED pattern of the 4P monolayer by means of one single reciprocal unit cell, see Fig. 1(b). The corresponding real space surface unit cell of the saturated 4P monolayer is in absolute values: $a=1.09\pm 0.01$ nm, $b=2.19\pm 0.01$ nm, $\gamma=74\pm 2^\circ$, $\Phi=37.5^\circ$. The quantities a , b , γ , and Φ are defined in Fig. 2. The matrix notation of this superstructure is

$$M = \begin{pmatrix} 8 & 1 \\ 2.75 & 4.5 \end{pmatrix}$$

(point-on-line commensurism).²⁴ The high symmetry of the Au(111) surface yields a total of 12 equivalent orientations of the 4P surface unit cell relative to the Au surface (domains).

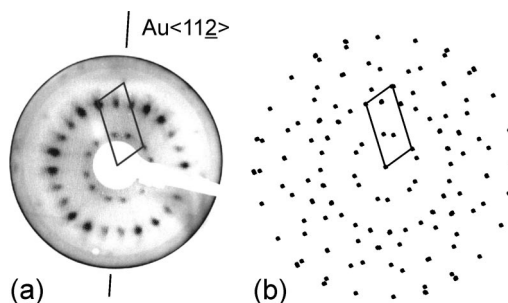


FIG. 1. (a) LEED image of the 4P monolayer on Au(111) at 16 V. The reciprocal surface unit cell is indicated by the parallelogram. The orientation of the Au(111) substrate is represented by the Au(112) direction. (b) Representation of the LEED pattern as obtained from a series of LEED images after correction for image deformation.

^{a)}Electronic mail: stefan.muellegger@tugraz.at

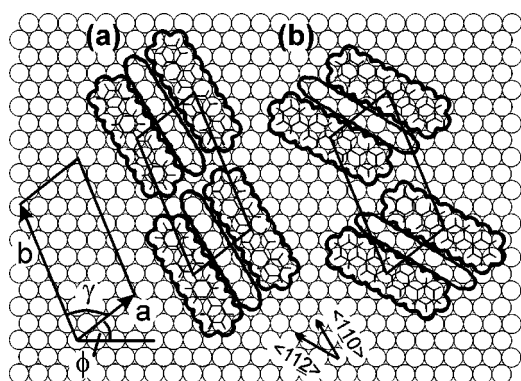


FIG. 2. Real space representation of the saturated 4P monolayer surface unit cell on a Au(111) surface. Two different arrangements of 4P (van der Waals size) relative to the Au(111) surface are shown: (a) azimuthal and (b) interazimuthal orientation, which correspond to the long molecular axes aligned parallel to the Au(1 $\bar{1}$ 0) and Au(11 $\bar{2}$) direction, respectively.

For the thick layers XRD-pole figures were taken of the five strongest reflections of 4P as determined from the monoclinic crystal structure of 4P.²¹ Figure 3 shows pole figures of the 211 and 201 reflections. A new software was developed to perform the indexation process.²³ Two different orientations of the 4P crystallites relative to the Au(111) substrate were found: 4P(211) and 4P(311) \parallel Au(111). Their relative proportion was determined on the basis of the observed pole densities: (211) was found twice as much as (311). Moreover, the indexation process yields the alignment of the 4P crystallites with respect to certain directions of the Au(111) surface (epitaxial relationship). For the (211) and (311) orientation we get: $[0\bar{1}1]_{4P} \parallel [53\bar{8}]_{Au}$ and $[\bar{1}30]_{4P} \parallel [3\bar{5}2]_{Au}$, respectively. Each of these two orientations exhibits 24 symmetrical equivalents, due to the substrate symmetry combined with the different growth possibilities of the 4P crystallites.

The 4P crystal structure²⁰ was used to determine the arrangement of the 4P molecules relative to the Au(111) surface. In case of the (211) orientation the aromatic planes of the 4P molecules are oriented parallel to the 4P(211) plane and hence to the Au(111) surface, see Fig. 4. The long molecular axes are aligned along azimuths (the Au(1 $\bar{1}$ 0) directions) or along interazimuths (the Au(1 $\bar{2}$ 1) directions). For (311), the aromatic planes are 7° off the Au(111) surface and the long molecular axes are tilted by 3° relative to the (inter)azimuthal direction. For both orientations, fractions of

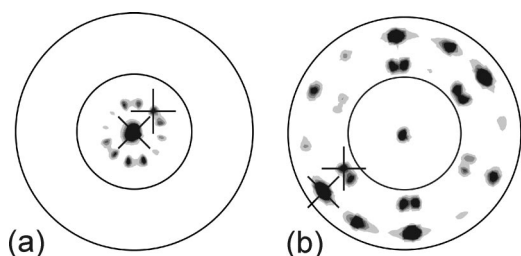


FIG. 3. Pole figures of the 211 (a) and 201 (b) reflection taken from a 200 nm 4P thin film. Dark areas represent directions of enhanced pole densities. The ψ limit of 20° and 40° are given by circles. The enhanced pole densities in the pole figures are assigned to orientations of 4P crystallites, examples for 4P(211) and 4P(311) \parallel to Au(111) are denoted by diagonal and straight crosses, respectively.

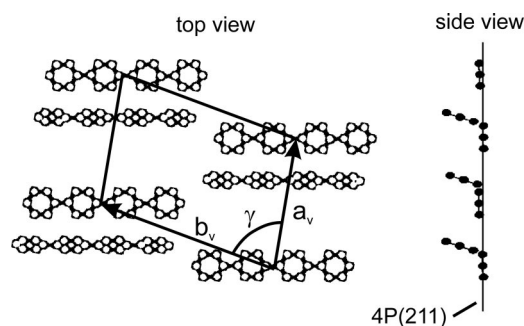


FIG. 4. Arrangement of the 4P molecules within the (211) plane (bulk phase) seen from top (left part) and along the direction of the long molecular axes (right part). The aromatic planes of the 4P molecules lie within the 4P(211) plane. The repeating unit is defined by a_v , b_v , and the cell angle, γ . Two orientations relative to the Au(111) surface were observed, where the long molecular axis is parallel to the Au(1 $\bar{1}$ 0) (azimuthal) or Au(11 $\bar{2}$) (interazimuthal) direction, respectively.

80% and 20% are found for azimuthal and interazimuthal alignment, respectively.

For films with different thickness, neither quantitative nor qualitative differences were observed by XRD. The 4P crystallites grow as needle-like islands and have a fixed crystallographic relationship with the Au(111) substrate. Therefore, the thin film can be interpreted as epitaxially grown.

Both azimuthal and interazimuthal molecular alignments within the 4P bulk phase are obviously caused by the geometry of the Au(111) surface (adsorbate–substrate interaction). Although we cannot derive any information about the molecular arrangement within the 4P monolayer directly from LEED measurements, it is obvious to assume that the molecular orientation is the same in the monolayer and the bulk phase. Therefore, we propose an arrangement of two 4P molecules per unit cell, with one molecule lying flat and the other one being side tilted (Fig. 2) and with the long molecular axes of the molecules oriented either azimuthally or interazimuthally. This molecular arrangement (two-dimensional space group: oblique $p2$) is corroborated by the following experimental facts: (1) In our thermal desorption measurements¹⁷ we observed two distinct monolayer adsorption states for the 4P molecules, suggesting the existence of two different binding states of the 4P molecules; (2) we compare the area of the 4P surface unit cell (2.3 nm^2 or 4×10^{13} unit cells/cm²) to the quantitative 4P coverage of the saturated monolayer (8×10^{13} molecules/cm² equal to $\sim 0.3 \text{ nm}$ mean thickness) measured with the quartz microbalance. This comparison suggests two molecules per surface unit cell; (3) the required van der Waals space of the two molecules per unit cell as well as the obvious similarity of this arrangement to the (211) orientation suggest a side tilt of one molecule, similar to 6P on Au(111) as observed by scanning tunneling microscopy (STM).¹³ As a matter of convention, these two types of differently bound molecules could be interpreted as “first and interstitial layer.”

The monolayer represents a prestage for the further 4P crystal growth. The 4P multilayer growth prefers the (211) orientation (Fig. 4), which is guided by that prestage, because the (211) plane shows a repeating unit very similar to the monolayer surface unit cell: $a_v = 1.38 \text{ nm}$, $b_v = 1.88 \text{ nm}$, and $\gamma = 79.3^\circ$. The (311) orientation is similar to (211) but there are small tilt angles of 7° for the aromatic

planes and 3° for the long molecular axis. The repeating unit of (311) is: $a_v = 1.87$ nm, $b_v = 1.88$ nm, and $\gamma = 76.9^\circ$. Presumably, the intermolecular forces between neighboring 4P molecules play a more important role in the formation of crystallites with the (311) orientation.

In conclusion, we have experimentally verified that quaterphenyl grows epitaxially on Au(111). The monolayer is governed by adsorbate–substrate interactions, leading to a regular structure with the molecules lying parallel to the surface and oriented either along the Au $\langle 1\bar{1}0 \rangle$ or the Au $\langle 11\bar{2} \rangle$ direction. This monolayer acts as a prestage of the further film growth, resulting in 4P crystallites with the (211) or (311) plane being parallel to the Au(111) surface. In both the monolayer and the multilayer islands, the 4P molecules exhibit the same well-defined orientation parallel to the Au $\langle 1\bar{1}0 \rangle$ and Au $\langle 11\bar{2} \rangle$ direction.

This work was supported by the Austrian FWF, Project No. P15625 and P15626.

¹S. R. Forrest, Chem. Rev. (Washington, D.C.) **97**, 1793 (1997).

²C. D. Dimitrakopoulos and D. J. Mascaró, IBM J. Res. Dev. **45**, 11 (2001).

³N. Karl, Synth. Met. **133–134**, 649 (2003).

⁴E. Umbach, K. Glöckler, and M. Sokolowski, Surf. Sci. **402–404**, 20 (1998).

⁵G. Witte and C. Wöll, Phase Transitions **76**, 291 (2003).

⁶F. Balzer and H.-G. Rubahn, Surf. Sci. **507–510**, 588 (2002).

⁷I. G. Hill, A. Kahn, Z. G. Soos, and R. A. Pascal, Chem. Phys. Lett. **327**, 181 (2000).

⁸H. Yanagi and S. Okamoto, Appl. Phys. Lett. **71**, 2563 (1997).

⁹D. J. Gundlach, Y. Y. Lin, T. N. Jackson, and D. G. Schlom, Appl. Phys. Lett. **71**, 3853 (1997).

¹⁰M. Era, T. Tsutsui, and S. Saito, Appl. Phys. Lett. **67**, 2436 (1995).

¹¹N. Koch, L. M. Yu, V. Parente, R. Lazzaroni, R. L. Johnson, G. Leising, J. J. Pireaux, and J. L. Bredas, Adv. Mater. (Weinheim, Ger.) **10**, 1038 (1998).

¹²S. Tasch, C. Brandstaetter, F. Meghdadi, G. Leising, G. Froyer, and L. Athouel, Adv. Mater. (Weinheim, Ger.) **9**, 33 (1997).

¹³C. B. France and B. A. Parkinson, Appl. Phys. Lett. **82**, 1194 (2003).

¹⁴S. Müllegger, O. Stranik, E. Zojer, and A. Winkler, Appl. Surf. Sci. (in press).

¹⁵J. V. Barth, H. Brune, G. Ertl, and R. J. Behm, Phys. Rev. B **42**, 9307 (1990).

¹⁶Ch. Wöll, S. Chiang, R. J. Wilson, and P. H. Lippel, Phys. Rev. B **39**, 7988 (1989).

¹⁷S. Müllegger, I. Salzmänn, R. Resel, and A. Winkler (unpublished).

¹⁸L. E. Alexander, in *X-Ray Diffraction Methods in Polymer Science* (R. E. Krieger, New York, 1979), pp. 209–240.

¹⁹H. E. Swanson and E. Tatge, Z. Angew. Phys. **8**, 202 (1956).

²⁰Y. Delugeard, J. Desuiche, and J. L. Baudour, Acta Crystallogr., Sect. B: Struct. Crystallogr. Cryst. Chem. **32**, 702 (1976).

²¹W. Kraus and G. Nolze, J. Appl. Crystallogr. **29**, 301 (1996).

²²S. Weber, J. Appl. Crystallogr. **29**, 306 (1996).

²³I. Salzmänn and R. Resel (unpublished).

²⁴D. E. Hooks, T. Fritz, and M. D. Ward, Adv. Mater. (Weinheim, Ger.) **13**, 227 (2001).